Available online at www.sciencedirect.com
ScienceDirect
International Journal of Pharmaceutics 344 (2007) 78–87
INTERNATIONAL JOURNAL OF PHARMACEUTICS
www.elsevier.com/locate/ijpharm

Tetrapyrrole-photosensitizers vectorization and plasma LDL: A physico-chemical approach

Stéphanie Bonneau [a,b,*], Christine Vever-Bizet [a,b], Halina Mojzisova [a,b], Daniel Brault [a,b]

[a] *Université Pierre et Marie Curie, Paris 6, UMR 7033, BioMoCeTi, Paris, F-75005, France*
[b] *CNRS, UMR7033, BioMoCeTi, Evry F-91000, France*

Received 6 February 2007; received in revised form 1 June 2007; accepted 6 June 2007
Available online 26 June 2007

Abstract

A photosensitizer is defined as a chemical entity able to induce, under light-irradiation effect, a chemical or physical alteration of another chemical entity. Thanks to their preferential retention in proliferating tissues, some photosensitizers are therapeutically used such as in photodynamic therapy (PDT). Besides, this method has already been approved for several indications. The selectivity of photosenzitizers for cells in proliferation involves both their association with low density lipoproteins (LDLs) and their ability to cross membranes under various pH conditions. The photosensitizers used are in most cases based on the porphyrin structure, but other compounds, of which far-red-light absorption properties are most compatible with biological tissues irradiation, have been developed, such as phthalocyanines. This paper presents physico-chemical studies of the interaction of a disulfonated aluminium phthalocyanine (AlPcS2) with human LDLs. The data obtained are compared with the parameters of the interaction of these lipoproteins with deuteroporphyrin (DP) and chlorin e6 (Ce6). A close attention is paid to the dynamic aspects of these phenomena. The data obtained on these simple systems then allowed us to interpret the sub-cellular localization of the photosensitizers on a human line of fibroblasts, and to evaluate the influence of LDLs on the intracellular distribution of the compounds. This last point is of major importance because the localization of such photosensitizers (in particular AlPcS2) in endocytic vesicles and their subsequent ability to induce a release of the contents of these vesicles – including externally added macromolecules – into the cytosol is the basis for a recent method for macromolecule activation, named photochemical internalization (PCI). PCI has been shown to potentiate the biological activity of a large variety of macromolecules. The comprehension of the mechanisms governing this particular sub-cellular localization could allow the design of better candidates for PCI.

Keywords: Vectorization; Photosensitizers; Low density lipoproteins (LDL); Sub-cellular localization; Photochemical internalization (PCI)

1. Introduction

With major advances in biotechnology, a variety of macromolecular therapeutic agents based on poly-nucleic or poly-amino acids has emerged as a powerful class of drugs that can provide solutions to many patho-physiological problems in medicine. Such therapeutic agents possess an enormous potential to complement or replace conventional pharmaceutical therapies that have been based traditionally on low molecular weight drugs. Their efficacy, however, requires appropriate delivery systems. Indeed, while they can quite easily reach extracellular targets, their great difficulty in reaching their intracellular targets severely limit the use of such molecules. In particular, the degradation of macromolecules in endocytic vesicles after their uptake by endocytosis is a major intracellular barrier for the therapeutic application of macromolecules having intracellular targets (Barbieri et al., 1993; Wu, 1997; Zabner et al., 1995). A new interesting approach for inducing the release of molecules from endocytic vesicles, based on the photodynamic destabilisation of their membrane, is called photochemical internalisation (PCI) (Berg et al., 1999, 2003; Selbo et al., 2001). The photodynamic effects are initiated by the absorption of light by a photosensitizer. This process leads a non-toxic molecule (photosensitizer) to produce short-lived reactive species, such as singlet oxygen or free radicals, under light excitation (Fig. 1). Owing to their brief lifetime, these active species diffuse less than 0.1 μm in a biological environment. Consequently, they can damage biomolecules only in the vicinity of the photosensitizer.

* Corresponding author at: Université Pierre et Marie Curie, Paris 6, UMR 7033, BioMoCeTi, Case courrier 138, 4 place Jussieu, 75252 Paris Cedex 05, France. Tel.: +33 1 40 79 36 97; fax: +33 1 69 87 43 60.
E-mail address: bonneau@mnhn.fr (S. Bonneau).

0378-5173/$ – see front matter © 2007 Elsevier B.V. All rights reserved.
doi:10.1016/j.ijpharm.2007.06.019

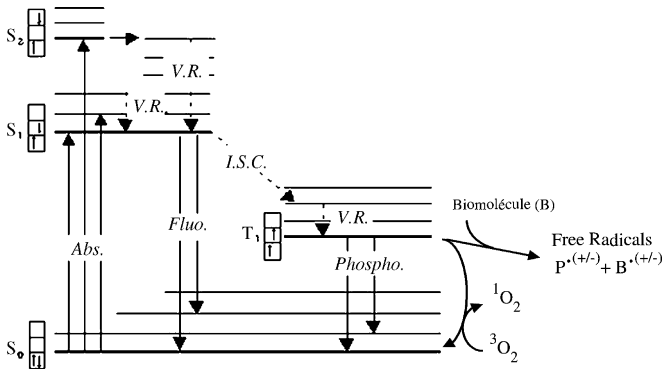

Fig. 1. Photodynamic processes: the Jablonski diagram shows the electronic states following absorption of light by a photosensitizer. The arrows represent the different processes (absorbtion: Abs.; fluorescence: Fluo.; phosphorescence: Phospho.; vibrational relaxation: V.R.). The excited singlet states of the photosensitizer are S1, S2, . . ., and the triplet state (T1) is obtained after intersystem crossing (ISC). The photochemical reaction pathways occur from the triplet state of a photosensitizer. Two reaction types are involved: a type I mechanism involving electron or hydrogen atom transfer from one molecule to the other and a type II mechanism involving energy transfer to molecular oxygen.

1.1. Photosensitizers, selectivity and photodynamic therapy (PDT)

The preferential retention of certain photosensitizers by tumors, as compared to normal surrounding tissues, has been recognized for many years. This specificity and the ability of these molecules to generate very-short-lived toxic species upon light irradiation are the basis of an anti-tumoral therapy, the photodynamic therapy (PDT) (Dougherty et al., 1998; Spikes, 1982). The light-induced molecular damage leads to the targeted cell's death. Only subcellular structures labeled by the photosensitizer are primarily damaged by the photodynamic processes. The intracellular localization of photosensitizers has thus a large influence on PDT effects, is well correlated with the phototoxicity and determines the mechanism of cell death (Hsieh et al., 2003; Kessel et al., 1997).

The mechanisms enhancing the retention of medically used photosensitizers are not fully clear, but some properties of the proliferating tissue seem to be of importance. The accumulation of photosensitizers may be favoured by the high number of LDL-receptors and/or by the low interstitial pH of targeted tissues (Gullino et al., 1965; Tannock and Rotin, 1989). Indeed, on the one hand, photosensitizers possess a high affinity for low-density lipoproteins (LDL) and the increased cholesterol catabolism of proliferating tissues leads to over-expression of LDL-receptors (Gal et al., 1981; Vitols et al., 1992). Hence, LDL could be natural carriers of photosensitizers and insure their targeting to tumor cells (Bonneau et al., 2002, 2004; Jori et al., 1984; Mojzisova et al., 2007; Silva et al., 2006). On the other hand, the tumor microenvironment, in particular the slightly acid pH of tumor extracellular medium could play an important role by governing the physico-chemical properties of photosensitizers (Cunderlikova et al., 1999, 2000). The importance of both these mechanisms is supported by the correlation established between the accumulation of photosensitizers in tumors and their structure, in particular their lipophilic character, the distribution of their polar and hydrophobic chains around the macrocycle and the electric charges of these chains (Ball et al., 1999; Boyle and Dolphin, 1996; Henderson et al., 1997).

In a recent period, PDT benefits from the development of laser and optical fibers and is now an established procedure for the treatment of some cancers (Dougherty et al., 1998; Pass, 1993). A first preparation, based on porphyrins, Photofrin®, has been approved since 1995 to treat some cancers. One of the disadvantages of such first-generation photosensitizers is their absorbance properties in a spectral-range where light is highly attenuated by tissues. A second generation of photosensitizers is being developed with improved light absorption in the red region (Boyle and Dolphin, 1996). Thus, molecules with larger macrocycle such as phthalocyanines have been synthetized. In parallel, PDT has found new applications to treat ophthalmic diseases (Ackroyd et al., 2001; Levy and Obochi, 1996). Most of therapeutically used photosensitizers have heterocyclic or porphyrin-like ring structures with conjugated double bonds (Moan et al., 1979; Niedre et al., 2003). In this paper, we will focus on three representative tetrapyrrol photosensitizers belonging to the major classes of medically used drugs: deuteroporphyrin, disulfonated aluminum phthalocyanine and chlorin e6 (Fig. 2). All these three molecules are amphiphilic with an asymmetrical repartition of the charged lateral chains. The charges of the porphyrin and of the chlorin can be neutralized, whereas those of the phthalocyanine cannot. The chlorin presents one more charge than the porphyrin, and the macrocycle of the phthalocyanine is larger than the others.

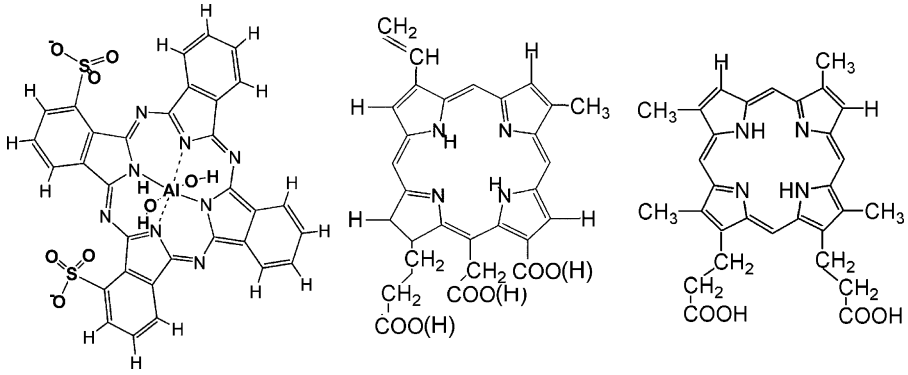

Fig. 2. Structures of disulfonated aluminum phthalocyanine (a), clorin e6 (b) and deuteroporphyrin (c).

1.2. Photosensitizers, selectivity and photochemical internalization (PCI)

The sub-cellular localization of photosensitizers is also of major importance for PCI applications. Indeed, PCI is based upon the light activation of a photosensitizer specifically located in the membrane of endocytic vesicles inducing the destabilization of these membranes (Dietze et al., 2006; Engesaeter et al., 2006). Thereby endocytosed molecules can be released to reach their target before being degraded in lysosomes. Of course, the most important constraint of the PCI technology is that the other organelles must not be affected. The cell's death must not be induced and the sub-cellular localization of the photosensitizer and the light irradiation intensity must thus be controlled. It should be noted that a light-induced effect means that the biological activity of the photosensitizers can be triggered at specific sites in the body, simply by illuminating the relevant areas.

The present work aims at studying the interaction of a photosensitizer utilized for PCI, the disulfonated aluminium phthalocyanine, with LDL. The physico-chemical parameters are compared with those obtained for deuteroporphyrin and chlorin e6 and the LDL-delivery influence on photosensitizers' cellular distribution is evaluated. A particular focus is given to the kinetics of these interactions in order to apprehend the possible influence of the tumor microenvironment.

2. Materials and methods

2.1. Chemicals

All the experiments were carried out at pH 7.4 in phosphate buffer saline (PBS 20 mM Na_2HPO_4, KH_2PO_4, 150 mM NaCl). Disulfonated aluminum phthalocyanine (AlPcS2, Fig. 2a) was prepared and characterized as described elsewhere (Ambroz et al., 1991; Bishop et al., 1993). The *cis*-isomer, i.e. the α,α-disubstituted regioisomer with the sulfonated groups on adjacent isoindole units, was isolated using reverse phase HPLC. Chlorin e6 (Ce6, Fig. 2b) was purchased from Porphyrin Products, Logan (UT, USA). Deuteroporphyrin (DP, Fig. 2c) was prepared as described previously (Brault et al., 1986). The photosensitizer solutions were handled in the dark to avoid any photobleaching.

Human low density lipoproteins (LDLs) were purchased from Calbiochem (San Diego, CA, USA). They were conditioned at a concentration of 9.52 mg/ml (protein content) in 150 mM NaCl pH 7.4 aqueous solution with 0.01% EDTA. Human serum albumin (HSA) essentially fatty acid free was purchased from Sigma (Saint Louis, Missouri, USA), and stored at 4 °C.

2.2. Steady state fluorescence measurements

Emission and excitation fluorescence spectra were recorded at 20 °C using an Aminco-Bowman 2 spectrofluorimeter (Edison, NJ). Recording was generally started 2 min after the preparation of the solutions under study. Data were fitted by using the Kaleidagraph software (Synergy Software, Reading, PA). The Levenberg–Marquard algorithm was used for non-linear curve fitting. The Mathcad software (Mathsoft, Inc., Cambridge, MA) was used for numerical simulations of phthalocyanine binding to LDL.

2.3. Kinetic measurements

2.3.1. Stopped-flow apparatus

The kinetics measurements were performed at 20 °C by using an Applied Photophysics (Leatherhead, UK) stopped-flow apparatus with mixing time of 1.2 ms. The mixing ratio was 1/1. The excitation light provided by a 150 W xenon arc lamp was passed through a monochromator with slits generally set to give a bandwidth of 4.65 nm. Fluorescence emission was collected using a low-cut filter (Oriel, France). The fluorescence signal was fed into a RISC workstation (Acorn Computers, UK) and analyzed using the software provided by the manufacturer. Slow kinetics measurements were performed by the Aminco Bowman spectrofluorimeter.

2.3.2. Theoretical models

Experimental results led us to consider two classes of photosensitizers bound to LDLs (defined as "class P" and "class L"). According to our experimental conditions (LDLs in excess), the pseudo-first-order approximation was assumed. Also, the two binding classes are considered to be independent.

$$P_F + \mathrm{LDL} \underset{k_{dP}}{\overset{k_{aP}}{\rightleftarrows}} P_P$$

$$P_F + \mathrm{LDL} \underset{k_{dL}}{\overset{k_{aL}}{\rightleftarrows}} P_L$$

The photosensitizer is designed by P. The constants k_{aP} and k_{dP} correspond to the association and dissociation rate constants for the "class P" (apoprotein) sites, k_{aL} and k_{dL} are those for photosensitizer binding to the lipid phase ("class L"). P_F stands for the free photosensitizer in aqueous solution.

The set of differential equations describing the system is:

$$\frac{dP_F}{dt} = k_{dL}P_L + k_{dP}P_P - (k'_{aL} + k'_{aP})P_F \quad (1a)$$

$$\frac{dP_L}{dt} = k'_{aL}P_F - k_{dL}P_L \quad (1b)$$

$$\frac{dP_P}{dt} = k'_{aP}P_F - k_{dP}P_P \quad (1c)$$

where k'_{aP} and k'_{aL} are apparent association rate constants as functions of the LDL concentration according to:

$$k'_{aL} = k_{aL} \times \mathrm{LDL}$$

$$k'_{aP} = k_{aP} \times \mathrm{LDL}$$

The model describing the DP-LDL association is based on approximations which have been fully described elsewhere (Bonneau et al., 2002) but cannot be extended here. For association of AlPcS2 to LDL, a bi-exponential signal is thus expected,

according to the following equation:

$$P_F = A_0 - A_1 \times \exp(-k_1 \times t) - A_2 \times \exp(-k_2 \times t) \quad (2a)$$

The rate constants k_1 and k_2 (abbreviated $k_{1,2}$) are:

$$k_{1,2}=\frac{1}{2}\left[\sum k \pm \sqrt{\left(\sum k\right)^2 - 4(k_{dP}k_{dL} + k'_{aL}k_{dP} + k'_{aP}k_{dL})}\right] \quad (2b)$$

where

$$\sum k = k_{dP} + k'_{aP} + k_{dL} + k'_{aL}$$

The amplitudes of the different terms are:

$$A_0 = P_{F(t=0)}\frac{k_{d_1}k_{d_2}}{k_1 k_2}$$

$$A_1 = P_{F(t=0)}\frac{(k_1)^2 - k_1(k_{dP} + k_{dL}) + k_{dP}k_{dL}}{k_1(k_2 - k_1)}$$

$$A_2 = P_{F(t=0)}\frac{(k_2)^2 - k_2(k_{dP} + k_{dL}) + k_{dP}k_{dL}}{k_2(k_1 - k_2)}$$

The amplitude ratio is given by:

$$\frac{A_2}{A_1} = \frac{(k_2)^2 - k_2(k_{dP} + k_{dL}) + k_{dP}k_{dL}}{(k_1)^2 - k_1(k_{dP} + k_{dL}) + k_{dP}k_{dL}} \quad (3)$$

In addition, in our previous paper (Bonneau et al., 2002) we have designed a method based on the transfer of photosensitizers from LDL to HSA allowing further estimate of the rate constants. The transfer of the photosensitizers from preloaded LDL to HSA was assumed to occur via the aqueous phase. The expected experimental signal is a bi-exponential, giving a direct access to the dissociation rate constants from "class P" and "class L" binding:

$$k_1 = k_{dP} \quad (4a)$$

$$k_2 = k_{dL} \quad (4b)$$

2.3.3. Analysis of the kinetics data

The analysis of the experimental bi-exponential curves (direct association of P to LDLand P transfer from LDL to HSA) using the software provided by the manufacturer gives access to the experimental rate constants. Eqs. (4a) and (4b) give two possible attributions for k_{dP} and k_{dL} values. Data obtained for the direct association were then fitted (by Eq. (2b)) according with these two possible attributions of k_{dP} and k_{dL}. It is to be noted that the Eq. (2b) has an important number of unknown parameters (k_{aP}, k_{dP}, k_{aL} and k_{dL}) that must be reduced to permit a significant non-linear regression. Thus, to reduce the degree of freedom, the two values attributed to k_{aP} and k_{dP} (or the inverse) have to be known. The study of the kinetics of the transfer from preloaded LDL to HSA has to be performed before the analysis of the P-LDL association data. The association rate constants were thus attributed, and the ambiguity for dissociation rate constants has been solved by the fact that one of the two possible attributions proved to be incompatible with our experimental results (see Section 3).

To further sustain the above models and the approximations made to analyze data, the kinetics of the interactions of the porphyrin with LDLs and the kinetics of the transfer of the porphyrin from LDLs to albumin were simulated by using the Mathcad mathematical software. The program involves the original set of differential equations without any assumptions and does not presuppose pseudo-first-order conditions.

2.4. Cell culture and experiments

2.4.1. Cell culture and treatments

Cells from the human fibroblast cell line HS68 were grown at 37 °C in DMEM (Dulbecco's Minimum Eagle Medium) supplemented with 10% fetal calf serum (FCS) and 100 U/mol Penicillin/Streptomycin in a fully humidified atmosphere of 5% C02 in air. The cells were passaged every 6 days and used between the 13th and the 19th passages.

For the microscopy experiments, the cells were seeded at 10,000 cells/ml on a 0.17 mm thick cover glass 48 h before experiments. Then, the cover glass was washed with Hank's balanced salt solution (HBSS) and the cells incubated with the photosensitizer in the same medium for 15 min at 37 °C. For each photosensitizer (AlPcS2, Ce6 or DP), two different types of experiments were performed: the photosensitizers were used alone or preloaded on LDL. In the second experiment series, the photosensitizers were first incubated with LDL for 15 min. As inferred from the kinetics experiments described in Section 3, this time is sufficient to achieve loading of LDLs with the photosensitizers. A third series, used as control, involved experiments carried out by using the same protocol but without photosensitizer. In all cases, after incubation, the cells were washed twice with HBSS.

2.4.2. Fluorescence microscopy

Microscope experiments were made by using a Nikon Eclipse TE 300 DV inverted microscope with an 100× oil objective. Appropriate fluorescence emission filters were used. Image acquisition was obtained with a back-illuminated cooled detector (CCD EEV: NTE/CCD-1024-EB, Roper Scientific, France). Data acquisition, processing and analysis were performed with Metamorph software, supplied by Universal Imaging Corporation (Roper Scientific, France).

After cell treatments, the red fluorescence emission of the photosensitizers was collected through a bandpass filter (645 ± 75 nm, Omega). A bandpass filter (330–380 nm) and a dichroic mirror at 400 nm were used for excitation. For all the experiments, this wavelength range was found to provide sufficient emission signals for photosensitizers as well as for the organelle-specific probe LysoTracker® green (Molecular Probes). This makes it possible to excite the photosensitizer and the organelle probe without changing the excitation set-up, minimizing the delay between fluorescence image acquisitions.

In the cases where LysoTracker® green was used to check lysosomal localization of the photosensitizer, the samples were washed twice and incubated 30 min with LysoTracker® green

Table 1
Affinity constants of the deuteroporphyrin, the chlorin e6 and the disulfonated phthalocyanine for LDL

n_P	K_{Pi}	K_P	K_L
Deuteroporphyrin (DP)			
4	$(8.8 \pm 0.2) \times 10^7\ M^{-1}$ K_{LDL} $(5.8 \pm 1.2) \times 10^8\ M^{-1}$	$(3.5 \pm 0.8) \times 10^8\ M^{-1}$ [a]	$(2.3 \pm 0.4) \times 10^8\ M^{-1}$
Disulfonated aluminium phthalocyanine (AlPcS2)			
5	$(1.2 \pm 0.2) \times 10^7\ M^{-1}$ K_{LDL} $(6.3 \pm 1.3) \times 10^7\ M^{-1}$	$(5.9 \pm 1.0) \times 10^7\ M^{-1}$ [a]	$(4.3 \pm 0.3) \times 10^6\ M^{-1}$
Clorin e6 (Ce6)			
10	$(5.0 \pm 0.6) \times 10^6\ M^{-1}$ K_{LDL} $(5.7 \pm 1.0) \times 10^7\ M^{-1}$	$(5.0 \pm 0.6) \times 10^7\ M^{-1}$ [a]	$(7.0 \pm 0.4) \times 10^6\ M^{-1}$

Data for the interactions between deuteroporphyrin and LDL are taken from (Bonneau et al., 2002) and those for the Ce6-LDL interaction from (Mojzisova et al., 2007). The values for the interactions of AlPcS2a with LDL were obtained in the present study.
[a] Indicates the experiments where the LDL fluorescence was followed.

(200 nM) before incubation with the photosensitizer. A bandpass filter (535 ± 45 nm, Omega) was used to isolate the green fluorescence emission of the probe. The emission wavelengths of photosensitizers and LysoTracker® green were different enough to allow their successive monitoring by using green and red bandpass filters, respectively. Moreover, the fluorescence emission band of LysoTracker® green corresponds to a region without significant absorption of photosensitizers. This makes unlikely any nonradiative energy transfer from the organelle probe to the photosensitizer in colocalization experiments.

3. Results and discussion

3.1. Physicochemical parameters of the interaction of photosensitizers with LDLs

3.1.1. Affinity of photosensitizers for LDLs

The affinity of AlPcS2 for LDL was studied with the method developed in our laboratory for the DP-LDL interactions (Bonneau et al., 2002). This approach is based upon the recording of both the fluorescence changes of the photosensitizers and those of the LDLs induced by the interaction. This method allows a clean differentiation between binding to the apoprotein and incorporation of the photosensitizers into the lipidic phase of LDLs. This parameter could be crucial, because the recognition of the LDLs by the cells, resulting in the endocytosis of the lipoprotein and its contents, involves the specific interaction of the apoprotein with the B/E-receptor. Therefore, the integrity of the apoprotein must be preserved.

As for deuteroporphyrin and chlorin e6 (Bonneau et al., 2002; Mojzisova et al., 2007), the disulfonated aluminium phthalocyanine is known to have a high affinity for LDLs (Bonneau et al., 2004) (see Table 1). The involvement of apoB in this interaction has been investigated here (Fig. 3). The binding of AlPcS2 on the proteic part of LDLs ("class P" binding) involves only five sites whereas the over-all saturation of LDLs, corresponding to the plateau of the inset, gives a saturation number at 7 AlPcS2 molecules per LDL. Two AlPcS2 molecules bound to the LDLs

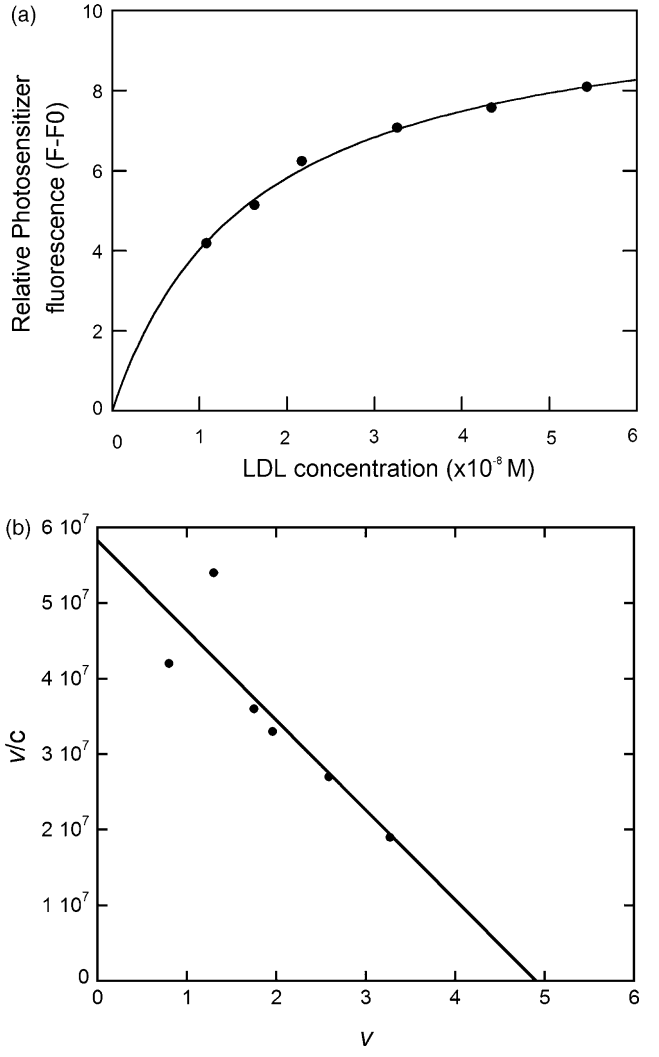

Fig. 3. Association of disulfonated aluminium phthalocyanine to LDL. (a) Quantification of the overall association ("class P" and "class L") by following the changes of phthalocyanine fluoresecnce intencity. (b) Quantification of binding of AlPcS2 to "class P" sites on LDL followed by changes of LDL intrinsic fluorescence at 330 nm (excitation wavelength 280 nm). The Scatchard plot is obtained from data computed according to the Halfman and Nishida method (see Bonneau, 2000).

are not associated with "class P" sites. This fixation corresponds to the incorporation of these two molecules in the lipids of LDLs ("class L" fixation). Although the number of "class P" binding is small, it is the prevailing process for AlPcS2–LDL association. However, it is expected that the recognition of LDLs by cellular receptors should not be impaired by the fixation of only five molecules. As a matter of fact, the recognition of LDL by cells is not modified by the association of porphyrins or chlorins e6 (de Smidt et al., 1993; Schmidt-Erfurth et al., 1997), although the interaction involves respectively 4 and 10 "class P" sites (Bonneau et al., 2002; Mojzisova et al., 2007).

For AlPcS2, the intrinsic affinity per "class P" site was found to be $K_{Pi} = 1.2 \times 10^7\ M^{-1}$, and the total affinity constant $K_{LDL} = 6.33 \times 10^7\ M^{-1}$. It is to be noted that the affinity constant corresponding to the association of AlPcS2 to the lipids of LDL is lower ($K_L = 4.3 \times 10^6\ M^{-1}$). This value is one order of magnitude smaller than the K_L value of DP (see Table 1). Surprisingly, in spite of its large hydrophobic macrocycle, the phthalocyanine is slightly associated to the LDL lipid phase, what has been suggested elsewhere (de Vries et al., 1999; Posse De Chaves et al., 2000). The affinity of AlPcS2 for phospholipid vesicles (DMPC) has been studied previously (Maman et al., 1999). The affinity constant obtained was $2.7 \times 10^6\ M^{-1}$ (expressed per phospholipid mole). On the basis of the number of phospholipids at the LDL-surface, a comparison can be done. The K_L value, expressed per phospholipid mole, is around $5 \times 10^3\ M^{-1}$. This value is two orders of magnitude smaller than expected. This could be explained by the high content in cholesterol of the LDLs and/or by the presence of non-neutralizable charges on the lateral chains of AlPcS2. Indeed, these charges are likely to limit the AlPcS2 incorporation in the hydrophobic core of LDLs' lipids and to favour the interaction with polar residues of apoB (i.e. favour "class P" fixation and decrease the "class L" association). As a matter of fact, it should be noted that the K_L value of AlPcS2 is not so different from that of Ce6, which possesses one more charge than DP.

However, in the case of the porphyrin as well as the chlorin, the K_L values in vesicles and in LDLs are in good agreement (Maman et al., 1999; Mojzisova et al., 2007). The lower value for AlPcS2, can then be explained by the larger size of the macrocycle, which facilitates the insertion of the molecule into the lipid bilayer of the vesicles but prevents its incorporation into the lipid monolayer on the surface of LDLs. In both cases, the presence of charges on lateral chains limits the association with the lipids.

3.1.2. Dynamics of the LDL–photosensitzier interaction

In order to better characterize the LDL–AlPcS2 interaction and to apprehend the potential effects of the microenvironment modifications in tumors on LDL-mediated vectorization of photosensitizers, kinetics parameters are considered now. Two different experiment types have been performed and analysed according to the theoretical model developed in the paragraph on methods. In these experiments, the binding capacity of the LDLs greatly exceeds the number of bound molecules and the kinetics were considered to obey pseudo-first order conditions. In both cases, the experiments involved the recording the fluorescence changes of AlPcS2 induced by the modification of its environment (when associated to HSA, to LDL or free in aqueous solution). The recorded signal always corresponds to the average of 10 shoots. These two types of measurements give us access to both the association and dissociation rate constants.

The first type of experiment has given a direct access to the exit rate constants from "class P" and "class L" fixation, k_{dP} and k_{dL}. A solution of lipoproteins (7.5×10^{-8} M) preloaded with AlPcS2 (2.2×10^{-8} M) was mixed, in the stopped-flow apparatus, with albumin (1×10^{-4} M) that possesses a good affinity for AlPcS2 (Ambroz et al., 1994). Rate constants of 6.8 and $0.8\ s^{-1}$ were obtained from the fit. They can be attributed to the release of the phthalocyanine from two types of sites on LDLs, in agreement with results obtained for the steady state and entrance studies.

Secondly, we mixed an AlPcS2 solution (4.4×10^{-8} M after mixing) with various LDL solutions (final concentrations 0.5, 0.75, 1, 1.25, 1.5×10^{-7} M). The signal was nicely fitted by a bi-exponential curve, in agreement with the two different classes of binding ("class P" and "class L") evidenced above. The binding process was really fast. The experimental rate constants k_1 and k_2 and the amplitude ratio A_2/A_1 were plotted versus LDL concentration in Fig. 4. These plots are adjusted with the aid of Eq. (2b) and Eq. (3), respectively. For these non-linear regression, two attributions of the experimental dissociation rate constants for "class P" and "class L" sites are possible: $k_{dP} = 6.8\ s^{-1}$ and $k_{dL} = 0.8\ s^{-1}$, or the inverse one. In fact the k_{dP} value is $0{,}8\ s^{-1}$ and k_{dL} is $6.8\ s^{-1}$. The inverse attribution is not compatible with our experimental results, i.e. no fit is possible with Eq. (2b). Moreover, the amplitude of the second exponential phase decreases when the LDL concentration increases, as expected from Eq. (3) (Fig. 4). In this figure, the curve corresponds to the best simulation on the MathCad software, by using the parameters determined from the best fit of kinetics.

All the rate constants, deduced from the two kinetics experiment types, are reported in Table 2. The association affinity constants were calculated ($K = k_a/k_d$). They are in good agreement with those determined by steady-state measurements.

The major contribution in the AlPcS2–LDL interaction arises from the "class P" sites. In order to better apprehend the nature of this binding, the related association rate constant can be compared to that of a process limited by diffusion of these species in solution. The theoretical limit is given by:

$$k_d = 4\pi(R_{LDL} + R_P)(D_{LDL} + D_P)N$$

where R_{LDL} and R_P are the radii of the LDL and phtahlocyanine, and D_{LDL} and D_P are the diffusion coefficients of LDL and phthalocyanine, respectively (Connors, 1990); N is Avogadro's number. The diffusion coefficient of phthalocyanine was estimated to be $(1\text{–}1.5) \times 10^{-10}\ m^2\ s^{-1}$ (Vever-Bizet and Brault, 1993) thanks to the porphyrin's diffusion coefficient and taking into account the size of the molecule. The diffusion of LDL is much slower, with a D_{LDL} value of $2 \times 10^{-11}\ m^2\ s^{-1}$ (Lee and Alaupovic, 1974). The radius of LDL is taken as 11×10^{-9} m (Schumaker et al., 1994; Segrest et al., 2001). The radius of phthalocyanine is 8×10^{-10} m. By using the above equation with appropriate unit conversion, the diffusion limit is

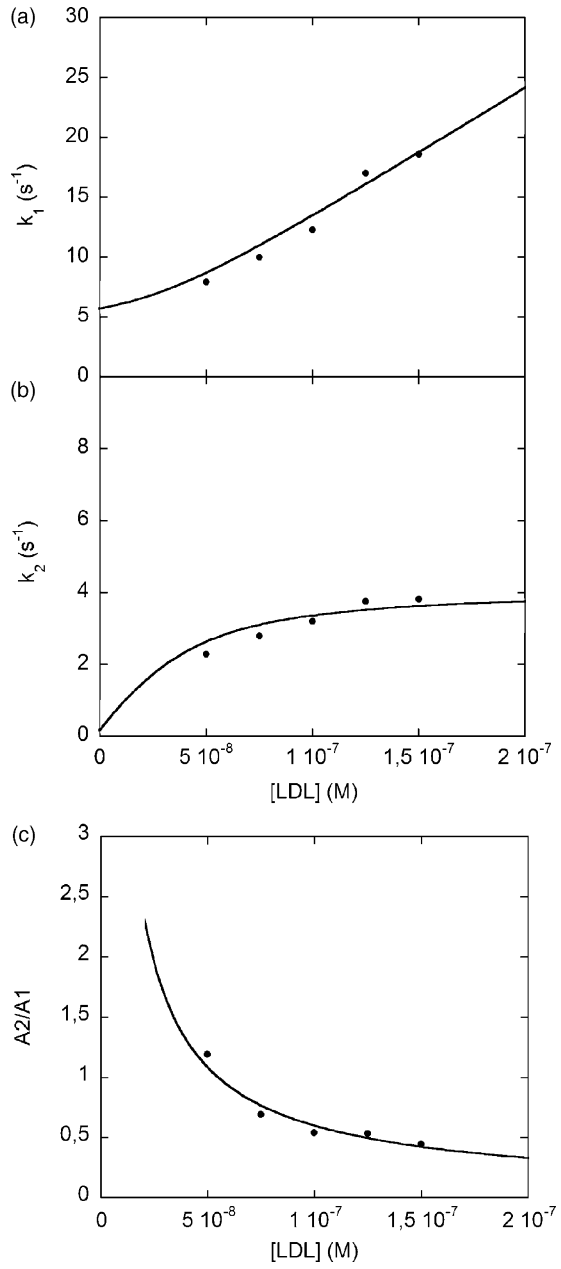

Fig. 4. Experimental rate constants, k_1 (a) and k_2 (b), of the AlPcS2–LDL association. (c) Amplitude ratio between slow and fast phases of the kinetics of AlPcS2–LDL association.

calculated to be $k_D = 1.1 \times 10^{10}\,M^{-1}\,s^{-1}$. The association rate constant experimentally determined is $5 \times 10^7\,M^{-1}\,s^{-1}$. This value is relatively far from that of the diffusion limited process. However, this binding involves only five well-defined sites, certainly with sizes of the same order of magnitude than that of the phthalocyanine. Thus, this lower value is expected.

Furthermore, k_{aL} expressed per phospholipids mole is $4.4 \times 10^4\,M^{-1}\,s^{-1}$. This value is relatively close to the one obtained with vesicles, $1.37 \times 10^5\,M^{-1}\,s^{-1}$. The small difference can be easily explained by the cholesterol content of the LDLs. This indicates that the dynamics of association of the AlPcS2 molecules is not really modified while the dissociation is greatly favoured in LDLs as compared with vesicles. This observation is in good agreement with the above hypothesis saying that the penetration of the AlPcS2 molecules in the phospholipid monolayer on the LDL-surface is limited either by the obstruction due to the macrocycle size, or by the non-neutralizable charges of the lateral chains.

Table 2
Values of equilibrium and rate constants of association of disulfonated aluminium phthalocyanine with the low-density lipoproteins ($n_p = 5^{b,b*}$)

Kinetics constants	
k_{aPi}	$(1.0 \pm 0.1) \times 10^7\,M^{-1}\,s^{-1}$ [a]
k_{aP}	$(5.0 \pm 0.5) \times 10^7\,M^{-1}\,s^{-1}$ [a]
k_{dP}	$0.8 \pm (0.1)\,s^{-1}$ [a]
k_{aL}	$(3.5 \pm 0.4) \times 10^7\,M^{-1}\,s^{-1}$ [a]
k_{dL}	$6.8 \pm 0.3\,s^{-1}$ [a]
Equilibrium constants	
K_{Pi}	$(1.2 \pm 0.27) \times 10^7\,M^{-1}$ [a], $(1.2 \pm 0.2) \times 10^7\,M^{-1}$ [b]
K_P	$(6.25 \pm 1.41) \times 10^7\,M^{-1}$ [a], $(5.9 \pm 1.0) \times 10^7\,M^{-1}$ [b*]
K_L	$(5.00 \pm 0.79) \times 10^6\,M^{-1}$ [a], $(4.3 \pm 0.3) \times 10^6\,M^{-1}$ [b]
K_{LDL}	$(6.3 \pm 1.3) \times 10^7\,M^{-1}$ [b], $(6.76 \pm 1.49) \times 10^7\,M^{-1}$ [a]

[a] Values calculated from the kinetics experiments and the corresponding simulations. The equilibrium constant are calclated according with $K = k_a/k_d$.
[b] Values calculated from steady-states measurements.
[b*] Indicates the experiments where the LDL fluorescence was followed.

3.2. Cellular localization of the photosensitizers

HS68 cells have been incubated with photosenstitizers (preloaded or not on LDL) solutions. The concentration of Ce6 was adjusted to 5×10^{-7} M. In a previous study, the same experiments were performed with DP and AlPcS2 concentrations adjusted to [DP] = 2.5×1^{-7} M and [AlPcS2] = 1×10^{-6} M. The differences in concentration compensate differences of fluorescence intensity. In all cases, the LDL concentration used for preloading (1×10^{-7} M) is sufficient to permit the fixation of almost all the photosensitizer molecules.

After 15 min of incubation of cells with one of these solutions, the fluorescence of the photosensitizer allows to determine its cellular localization. The results are depicted in Fig. 5. A particular attention is paid to the possible influence of LDLs. For DP, the fluorescence was found to be diffuse, suggesting a membrane and cytosol localization (Bonneau et al., 2004). The distribution of the porphyrin was not modified by its vectorization by LDLs. These results can be easily explained by the rapidity of the dynamics of the DP-LDL interaction and the high rate of diffusion of this molecule through membranes. Then, in spite of their high affinity for DP, LDLs only play a marginal role in the porphyrin cellular localization. However, this high affinity confers to LDLs an important role as porphyrin carriers in blood. Kinetics also suggest a high rate of exchange with other plasma proteins. We could imagine that LDLs efficiently carry DP, or related porphyrins, to the tumoral site where transfer to the cellular membrane occurs rapidly.

The phthalocyanine, on the contrary, was found to be mainly localized within intracellular vesicles, and the role of LDLs was major. Here, it is to be noted that the disulfonated groups of the phthalocyanine are permanently charged in cellular condi-

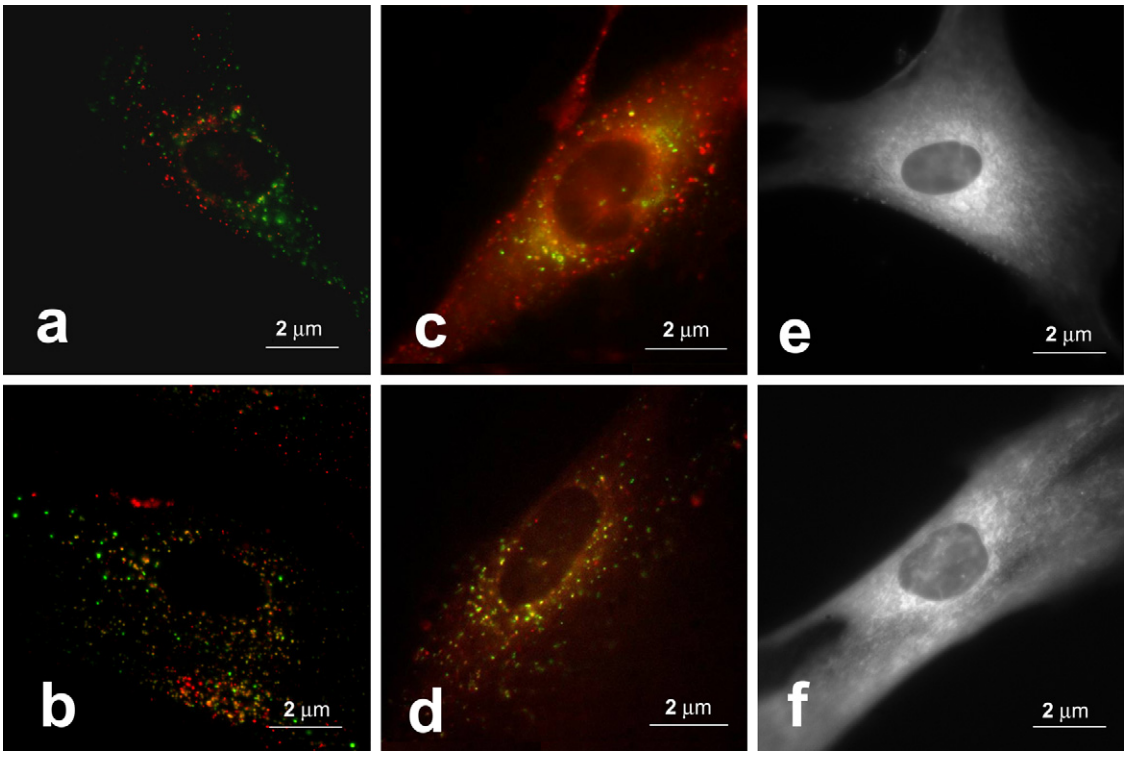

Fig. 5. Fluorescence microscopy experiments on HS68 fibroblasts: for (a), (b), (c) and (d), cells were pre-labeled with LysoTracker®. Fluorescence excitation: 330–380 nm. The red photosensitizer emission and the green LysoTracker1 emission were collected by using filters at 645 ± 75 and 535 ± 45 nm, respectively. The overlays of green and red images are shown. When the photosensitizer is localized into lysosomes, its co-localization with LysoTracker® is illustrated by yellow spots resulting from the overlay of red and green emissions. For DP, no co-localization experiments have been done, and thus only the red fluorescence was collected (e and f). The image is the depicted in grey levels reflecting the red fluorescence of the photosensitizer. Fluorescence microscopy study of the incorporation of AlPcS2 into HS68 fibroblasts: (a) cells incubated with AlPcS2 alone; (b) cells incubated with AlPcS2 pre-associated to LDL. Fluorescence microscopy study of the incorporation of Ce6 into HS68 fibroblasts: (c) cells incubated with Ce6 alone; (d) cells incubated with Ce6 pre-associated to LDL. Fluorescence microscopy study of the incorporation of DP into HS68 fibroblasts: (e) cells incubated with DP; (f) cells incubated with DP pre-associated to LDL.

tions of pH, whereas DP and Ce6 are weak acids. The AlPcS2 is not permeant through membranes, whereas DP, and to a lesser extent Ce6, are able to cross biological membranes and then to escape from endocytic vesicles, when incorporated by endocytosis. As shown by the co-localization with LysoTracker® green, the vectorization of the phthalocyanine by LDLs leads to a lysosomal localization resulting from a LDL-mediated endocytosis process. When AlPcS2 is not preloaded on LDL, incorporation by bulk endocytosis process is efficient, and most of the intracellular vesicles, where AlPcS2 are localized, are not lysosomes. Similar granular fluorescence pattern and lysosome localization of sulfonated porphyrins or phthalocyanines have been observed for various cell lines (Bonneau et al., 2004; Moan et al., 1994; Wessels et al., 1992) in agreement with their inability to cross membranes. Indeed, in that case, the photosensitizer is released from LDLs and stays in the lysosomal membrane that acts as a barrier. As compared with the DP case, the equilibrium between cells and LDLs is then balanced in favour of LDL–photosensitizer association. The major cellular incorporation process is thus endocytosis and the LDL influence is enhanced.

As expected, Ce6 was found to have an intermediate behaviour and a balanced influence of LDL on its localization. In absence of LDL, Ce6 is localized in the plasma membrane and in intracellular vesicles. The co-localization experiment shows that the most of these vesicles are not lysosomes. When Ce6 has been vectorized by LDLs the sub-cellular localization was different. The plasma membrane labelling was less visible and Ce6 was mainly located in intracellular vesicles, that were identified for the most part as lysosomes. The influence of the LDLs is thus well correlated with the importance of the endocytosis pathway (bulk or LDL-mediated) and depends on the rapidity of the dynamics of the LDL–photosensitizer interaction.

Acknowledgements

The authors thank David Phillips (Imperial College of Science, London) for a generous gift of the disulfonated aluminium phthalocyanine. The microscopy experiments were performed by using the apparatus installed at CEMIM, a division of the National Museum of Natural History (MNHN) under the guidance of Dr. Marc Gèze and Dr. Marc Dellinger. The stopped-flow apparatus was acquired thanks to subsidy from the charity associations ARC (grant # 7209).

References

Ackroyd, R., Kelty, C., Brown, N., Reed, M., 2001. The history of photodetection and photodynamic therapy. Photochem. Photobiol. 74, 656–669.

Ambroz, M., Beeby, A., MacRobert, A.J., Simpson, M.S., Svensen, R.K., Phillips, D., 1991. Preparative, analytical and fluorescence spectroscopic studies of sulphonated aluminium phthalocyanine photosensitizers. J. Photochem. Photobiol. B 9, 87–95.

Ambroz, M., MacRobert, A.J., Morgan, J., Rumbles, G., Foley, M.S., Phillips, D., 1994. Time-resolved fluorescence spectroscopy and intracellular imaging of disulphonated aluminium phthalocyanine. J. Photochem. Photobiol. B 22, 105–117.

Ball, D.J., Mayhew, S., Wood, S.R., Griffiths, J., Vernon, D.I., Brown, S.B., 1999. A comparative study of the cellular uptake and photodynamic efficacy of three novel zinc phthalocyanines of differing charge. Photochem. Photobiol. 69, 390–396.

Barbieri, L., Battelli, M.G., Stirpe, F., 1993. Ribosome-inactivating proteins from plants. Biochim. Biophys. Acta 1154, 237–282.

Berg, K., Prasmickaite, L., Selbo, P.K., Hellum, M., Bonsted, A., Hogset, A., 2003. Photochemical internalization (PCI)—a novel technology for release of macromolecules from endocytic vesicles. Oftalmologia 56, 67–71.

Berg, K., Selbo, P.K., Prasmickaite, L., Tjelle, T.E., Sandvig, K., Moan, J., Gaudernack, G., Fodstad, O., Kjolsrud, S., Anholt, H., Rodal, G.H., Rodal, S.K., Hogset, A., 1999. Photochemical internalization: a novel technology for delivery of macromolecules into cytosol. Cancer Res. 59, 1180–1183.

Bishop, S.M., Khoo, B.J., MacRobert, A.J., Simpson, M.S., Phillips, D., Beeby, A., 1993. Characterisation of the photochemotherapeutic agent disulphonated aluminium phthalocyanine and its high-performance liquid chromatographic separated components. J. Chromatogr. 646, 345–350.

Bonneau, S., Morliere, P., Brault, D., 2004. Dynamics of interactions of photosensitizers with lipoproteins and membrane-models: correlation with cellular incorporation and subcellular distribution. Biochem. Pharmacol. 68, 1443–1452.

Bonneau, S., Vever-Bizet, C., Morlière, P., Mazière, J.C., Brault, D., 2002. Equilibrium and kinetic studies of the interactions of a porphyrin with low density lipoproteins. Biophys. J. 83, 3470–3481.

Boyle, R.W., Dolphin, D., 1996. Structure and biodistribution relationships of photodynamic sensitizers. Photochem. Photobiol. 64, 469–485.

Brault, D., Vever-Bizet, C., Le Doan, T., 1986. Spectrofluorimetric study of porphyrin incorporation into membrane models—evidence for pH effects. Biochim. Biophys. Acta 857, 238–250.

Connors, K.A., 1990. Chemicals Kinetics. VCH Publishers, New York.

Cunderlikova, B., Gangeskar, L., Moan, J., 1999. Acid–base properties of chlorin e6: relation to cellular uptake. J. Photochem. Photobiol. B 53, 81–90.

Cunderlikova, B., Kongshaug, M., Gangeskar, L., Moan, J., 2000. Increased binding of chlorin e(6) to lipoproteins at low pH values. Int. J. Biochem. Cell Biol. 32, 759–768.

de Smidt, P.C., Versluis, A.J., van Berkel, T.J., 1993. Properties of incorporation, redistribution, and integrity of porphyrin-low-density lipoprotein complexes. Biochemistry 32, 2916–2922.

de Vries, H.E., Moor, A.C., Dubbelman, T.M., van Berkel, T.J., Kuiper, J., 1999. Oxidized low-density lipoprotein as a delivery system for photosensitizers: implications for photodynamic therapy of atherosclerosis. J. Pharmacol. Exp. Ther. 289, 528–534.

Dietze, A., Selbo, P.K., Prasmickaite, L., Weyergang, A., Bonsted, A., Engesaeter, B., Hogset, A., Berg, K., 2006. Photochemical internalization (PCI): a new modality for light activation of endocytosed therapeuticals. J. Environ. Pathol. Toxicol. Oncol. 25, 521–536.

Dougherty, T.J., Gomer, C.J., Henderson, B.W., Jori, G., Kessel, D., Korbelik, M., Moan, J., Peng, Q., 1998. Photodynamic therapy. J. Natl. Cancer Inst. 90, 889–905.

Engesaeter, B.O., Tveito, S., Bonsted, A., Engebraaten, O., Berg, K., Maelandsmo, G.M., 2006. Photochemical treatment with endosomally localized photosensitizers enhances the number of adenoviruses in the nucleus. J. Gene Med. 8, 707–718.

Gal, D., Ohashi, M., MacDonald, P.C., Buchsbaum, H.J., Simpson, E.R., 1981. Low-density lipoprotein as a potential vehicle for chemotherapeutic agents and radionucleotides in the management of gynecologic neoplasms. Am. J. Obstet. Gynecol. 139, 877–885.

Gullino, P.M., Grantham, F.H., Smith, S.H., Haggerty, A.C., 1965. Modifications of the acid-base status of the internal milieu of tumors. J. Natl. Cancer Inst. 34, 857–869.

Henderson, B.W., Bellnier, D.A., Greco, W.R., Sharma, A., Pandey, R.K., Vaughan, L.A., Weishaupt, K.R., Dougherty, T.J., 1997. An in vivo quantitative structure-activity relationship for a congeneric series of pyropheophorbide derivatives as photosensitizers for photodynamic therapy. Cancer Res. 57, 4000–4007.

Hsieh, Y.J., Wu, C.C., Chang, C.J., Yu, J.S., 2003. Subcellular localization of Photofrin determines the death phenotype of human epidermoid carcinoma A431 cells triggered by photodynamic therapy: when plasma membranes are the main targets. J. Cell Physiol. 194, 363–375.

Jori, G., Beltramini, M., Reddi, E., Salvato, B., Pagnan, A., Ziron, L., Tomio, L., Tsanov, T., 1984. Evidence for a major role of plasma lipoproteins as hematoporphyrin carriers in vivo. Cancer Lett. 24, 291–297.

Kessel, D., Luo, Y., Deng, Y., Chang, C.K., 1997. The role of subcellular localization in initiation of apoptosis by photodynamic therapy. Photochem. Photobiol. 65, 422–426.

Lee, D.M., Alaupovic, P., 1974. Physiocochemical properties of low-density lipoproteins of normal human plasma. Evidence for the occurrence of lipoprotein B in associated and free forms. Biochem. J. 137, 155–167.

Levy, J.G., Obochi, M., 1996. New applications in photodynamic therapy. Introduction. Photochem. Photobiol. 64, 737–739.

Maman, N., Dhami, S., Phillips, D., Brault, D., 1999. Kinetic and equilibrium studies of incorporation of di-sulfonated aluminum phthalocyanine into unilamellar vesicles. Biochim. Biophys. Acta 1420, 168–178.

Moan, J., Berg, K., Anholt, H., Madslien, K., 1994. Sulfonated aluminium phthalocyanines as sensitizers for photochemotherapy. Effects of small light doses on localization, dye fluorescence and photosensitivity in V79 cells. Int. J. Cancer 58, 865–870.

Moan, J., Pettersen, E.O., Christensen, T., 1979. The mechanism of photodynamic inactivation of human cells in vitro in the presence of haematoporphyrin. Br. J. Cancer 39, 398–407.

Mojzisova, H., Bonneau, S., Vever-Bizet, C., Brault, D., 2007. The pH-dependent distribution of the photosensitizer chlorin e6 among plasma proteins and membranes: a physico-chemical approach. Biochim. Biophys. Acta 1768, 366–374.

Niedre, M.J., Secord, A.J., Patterson, M.S., Wilson, B.C., 2003. In vitro tests of the validity of singlet oxygen luminescence measurements as a dose metric in photodynamic therapy. Cancer Res 63, 7986–7994.

Pass, H.I., 1993. Photodynamic therapy in oncology: mechanisms and clinical use. J. Natl. Cancer Inst. 85, 443–456.

Posse De Chaves, E.I., Vance, D.E., Campenot, R.B., Kiss, R.S., Vance, J.E., 2000. Uptake of lipoproteins for axonal growth of sympathetic neurons. J. Biol. Chem. 275, 19883–19890.

Schmidt-Erfurth, U., Diddens, H., Birngruber, R., Hasan, T., 1997. Photodynamic targeting of human retinoblastoma cells using covalent low-density lipoprotein conjugates. Br. J. Cancer 75, 54–61.

Schumaker, V.N., Phillips, M.L., Chatterton, J.E., 1994. Apolipoprotein B and low-density lipoprotein structure: implications for biosynthesis of triglyceride-rich lipoproteins. Adv. Protein Chem. 45, 205–248.

Segrest, J.P., Jones, M.K., De Loof, H., Dashti, N., 2001. Structure of apolipoprotein B-100 in low density lipoproteins. J. Lipid Res. 42, 1346–1367.

Selbo, P.K., Sivam, G., Fodstad, O., Sandvig, K., Berg, K., 2001. In vivo documentation of photochemical internalization, a novel approach to site specific cancer therapy. Int. J. Cancer 92, 761–766.

Silva, J.N., Filipe, P., Morliere, P., Maziere, J.C., Freitas, J.P., Cirne de Castro, J.L., Santus, R., 2006. Photodynamic therapies: principles and present medical applications. Biomed. Mater. Eng. 16, S147–S154.

Spikes, J.D., 1982. Photodynamic reactions in photomedicine. In: Regan, J.D., Parrish, J.A. (Eds.), The Science of Photomedicine. Plenum Press, New York, pp. 113–144.

Tannock, I.F., Rotin, D., 1989. Acid pH in tumors and its potential for therapeutic exploitation. Cancer Res. 49, 4373–4384.

Vever-Bizet, C., Brault, D., 1993. Kinetics of incorporation of porphyrins into small unilamellar vesicles. Biochim. Biophys. Acta 1153, 170–174.

Vitols, S., Peterson, C., Larsson, O., Holm, P., Aberg, B., 1992. Elevated uptake of low density lipoproteins by human lung cancer tissue in vivo. Cancer Res. 52, 6244–6247.

Wessels, J.M., Strauss, W., Seidlitz, H.K., Ruck, A., Schneckenburger, H., 1992. Intracellular localization of meso-tetraphenylporphine tetrasulphonate probed by time-resolved and microscopic fluorescence spectroscopy. J. Photochem. Photobiol. B 12, 275–284.

Wu, M., 1997. Enhancement of immunotoxin activity using chemical and biological reagents. Br. J. Cancer 75, 1347–1355.

Zabner, J., Fasbender, A.J., Moninger, T., Poellinger, K.A., Welsh, M.J., 1995. Cellular and molecular barriers to gene transfer by a cationic lipid. J. Biol. Chem. 270, 18997–19007.